XLVI CILAMCE
VITÓRIA - ES - BRAZIL - 2025
XLVI IBERO-LATIN AMERICAN CONGRESS ON COMPUTATIONAL METHODS IN ENGINEERING

Seat-induced vibration transmission to a biodynamic model in a freight vehicle

Jônatas S. Vianna[1], Rafael Ramanzini[1], Vitor S. Figueiredo[1], Lucas M. Visnievski[1], Walter J. Paucar Casas[1]

[1]*Department of Mechanical Engineering, Federal University of Rio Grande do Sul*
Rua Sarmento Leite 425, CEP 90050-170, Porto Alegre – RS, Brazil
jonatas.svianna@gmail.com, rafaelramanzini@gmail.com, vitor.siq.f@gmail.com, lucasmirandavis@gmail.com, walter.casas@ufrgs.br

Abstract. Prolonged exposure to mechanical vibrations in freight vehicles presents a health risk to drivers, as it can cause discomfort and fatigue without a proper seat. Knowledge of these vibrations is essential for their monitoring, control, and minimization. To this end, mathematical models are used to simulate the vibrational behavior of vehicles in interaction with biomechanical models of the human body. These simulations allows a dynamic analysis that enables the optimization of component design and manufacturing. The use of software such as MATLAB, for example, allows for mass-spring-damper modeling to represent both the vehicle and the human body. This makes it possible to understand how the masses of the biodynamic model behave when a truck moves on, for instance, through a C-Class road. Analyzing the propagation of vibrations from the seat to the driver's body, combined with numerical integration, mode shape evaluation, and frequency response analysis, provides a comprehensive approach to assess system performance. This methodology is fundamental for design optimization, as it enables the analysis of vibration behavior and consequently enhances driver comfort and safety.

Keywords: biodynamic modeling, mechanical vibration, human comfort.

1 Introduction

Prolonged exposure to mechanical vibrations while operating freight vehicles poses a substantial risk to the health and well-being of drivers and off-road vehicle operators. This issue is particularly critical during long work shifts, where continuous exposure can lead to a range of adverse effects, from simple discomfort and fatigue to the long-term development of musculoskeletal disorders.

To mitigate these vibrations, researchers, such as Kim *et al.* [1], analyze the transmissibility from the seat to the human body. In this context, understanding and controlling mechanical vibrations become essential not only for mitigating occupational risks but also for improving user safety and comfort.

Mathematical modeling and computational simulation are suitable tools for studying these vibrational dynamics. They enable a predictive and detailed analysis of the interaction between the vehicle and biomechanical models of the human body, providing critical insights for optimizing design and manufacturing processes before final solutions are implemented.

In this study, using MATLAB software, a multibody model was developed to simulate both the vehicle system and the driver. The research focuses on analyzing the biodynamic behavior of the driver through a 20-degree-of-freedom (DOF) model subjected to seat excitations. The objective of this work is to evaluate the transmissibility from the driver's seat to the head, assessing the vibration behavior in the human body. The biodynamic model is formulated following the proposal of Guruguntla and Lal [2]. The research's methodological scope is to investigate the propagation of vibrations, starting from the irregularities of a C-Class road, through the vehicle, to the various segmented regions of a biodynamic human model. In this case, the damping of the rear suspensions of both the truck and the cabin is considered to have a non-linear behavior, based on the approach proposed by Chen *et al.* [3].

The values obtained from this model are of great relevance as they provide information that can assist designers and engineers in the development and optimization of vehicle components. The conclusions of this study can contribute to the design of safer and more ergonomic vehicles, reducing the risks associated with vibration exposure and, consequently, promoting a healthier work environment for drivers.

2 Theoretical background

2.1 Dynamic system

The dynamic equations for the multi-body model of the truck and semi-trailer combination were formulated using the Lagrangian method. Based on the principle of virtual work, this method is an effective tool for dynamic modeling because it allows the equations of motion to be formulated with any set of independent generalized coordinates, according to eq. (1).

$$\frac{d}{dt}\left(\frac{\partial T}{\partial \dot{q}_i}\right) - \frac{\partial T}{\partial q_i} + \frac{\partial U}{\partial q_i} + \frac{\partial D}{\partial \dot{q}_i} = Q_i, \quad i = 1,2,\dots,n. \tag{1}$$

To formulate the dynamic equations for a system, one uses expressions for the kinetic energy (T), the potential deformation energy (U), the dissipation energy (D), and the generalized forces (Q) associated with a set of independent generalized coordinates (q_i). Based on the definition of these energies and forces, the equation allows for obtaining the system's equations of motion.

2.2 Numerical integration

The Newmark integration method is used to obtain the time-domain response at the driver's seat under Class C-road irregularities, as well as to determine the responses of the human body segments to the excitations transmitted through the seat.

The dynamic equilibrium equation, $\mathbf{M}\ddot{\mathbf{U}}^{t+\Delta t} + \mathbf{C}\dot{\mathbf{U}}^{t+\Delta t} + \mathbf{K}\mathbf{U}^{t+\Delta t} = \mathbf{R}^{t+\Delta t}$, is solved using the mass $\mathbf{M}$, stiffness $\mathbf{K}$, and damping $\mathbf{C}$ matrices, along with the external force vector $\mathbf{R}$. In the Newmark method, a sequence of substitutions is applied to express the acceleration and velocity at time $t + \Delta t$ in terms of the unknown displacement $\mathbf{U}^{t+\Delta t}$. Some parameters are established to initialize the method, according to eq. (2), which define the precision and numerical stability of the calculation. Subsequently, the integration constants in eqs. (3) and (4) are calculated based on these values.

$$\delta \geq 0.50 \quad \alpha \geq 0.25(0.5 + \delta)^2 \tag{2}$$

$$a_0 = \frac{1}{\alpha \Delta t^2}, \quad a_1 = \frac{\delta}{\alpha \Delta t}, \quad a_2 = \frac{1}{\alpha \Delta t}, \quad a_3 = \frac{1}{2\alpha} - 1 \tag{3}$$

$$a_4 = \frac{\delta}{\alpha} - 1, \quad a_5 = \frac{\Delta t}{2}\left(\frac{\delta}{\alpha} - 1\right), \quad a_6 = \Delta t(1 - \delta), \quad a_7 = \delta \Delta t \tag{4}$$

The effective stiffness matrix $\hat{\mathbf{K}}$ is formed using eq. (5). This consolidated matrix then simplifies the equations of motion for numerical solution.

$$\hat{\mathbf{K}} = \mathbf{K} + a_0\mathbf{M} + a_1\mathbf{C} \tag{5}$$

The effective load combines the external forces of the new time step with the effects of mass and damping from the previous time step. This load is then used to determine the displacement.

$$\hat{\mathbf{R}}^{t+\Delta t} = \mathbf{R}^{t+\Delta t} + \mathbf{M}\left(a_0\mathbf{U}^t + a_2\dot{\mathbf{U}}^t + a_3\ddot{\mathbf{U}}^t\right) + \mathbf{C}(a_1\mathbf{U}^t + a_4\dot{\mathbf{U}}^t + a_5\ddot{\mathbf{U}}^t) \tag{6}$$

With the effective load defined, the matrix equation in eq. (7) is solved using the triangularized effective stiffness matrix to obtain the displacement at the new time step.

$$\mathbf{L}\mathbf{D}\mathbf{L}^T\mathbf{U}^{t+\Delta t} = \hat{\mathbf{R}}^{t+\Delta t} \tag{7}$$

After that the equations update the system's accelerations and velocities for the new time step. These are computed based on the values from the previous time step and the integration constants.

$$\ddot{\mathbf{U}}^{t+\Delta t} = a_0(\mathbf{U}^{t+\Delta t} - \mathbf{U}^{t}) - a_2\,\dot{\mathbf{U}}^{t} - a_3\ddot{\mathbf{U}}^{t} \tag{8}$$

$$\dot{\mathbf{U}}^{t+\Delta t} = \dot{\mathbf{U}}^{t} + a_6\ddot{\mathbf{U}}^{t} + a_7\,\ddot{\mathbf{U}}^{t+\Delta t} \tag{9}$$

3 Methodology

3.1 Vehicle model

A 24-degree-of-freedom (DOF) multibody model was employed to represent a truck–semitrailer combination, as shown in Figure 1. Both units feature three axles and are connected by a fifth wheel, forming an articulated configuration that extends the two-dimensional model of Chen *et al.* [3]. The system is composed of lumped masses m, stiffness elements k, and damping coefficients c, which characterize the dynamic behavior of the suspension, tires, and structural components. The longitudinal geometric dimensions are defined by the variable l, whereas the vehicle widths are represented by e and a. The road surface irregularities are described by q. Subscripts L and R denote the left and right sides of the vehicle, respectively. Most geometric and physical parameter values are based on Chen *et al.* [3].

The distribution of the 24 DOFs was assigned to the main components of the system. The primary bodies, such as the chassis, cab, and semi-trailer, each have 3 DOFs corresponding to vertical x, pitch θ, and roll φ motions. Each of the six axles in the system has 2 DOFs, representing vertical and roll motions. The driver's seat has 1 DOF associated with vertical motion. The truck's rear suspensions, which form a balanced system, are modeled with 2 DOFs per side, describing the vertical motion and pitch of the leaf spring assemblies.

The model incorporates nonlinear damping forces in the rear suspensions of the cab and chassis, reflecting the real dynamic behavior observed experimentally in the work of Chen *et al.* [3]. In contrast, the semi-trailer suspensions and the front suspensions of the cab and chassis are modeled with linear damping. The rear suspension of the cab uses a special configuration of dampers and springs acting in both the vertical and longitudinal directions.

The vehicle is subjected to a virtual Class C road profile standardized by ISO 8608:2016, featuring phase-shifted profiles with cross-correlation. This type of road profile can be used for computational road simulations following a PSD-based approach, as proposed by Múčka [4]. The dynamic behavior is evaluated considering only straight-path motion, excluding lateral forces and cornering effects.

The main simplifications adopted in the model include point contact between the tires and the road, without separation; the assumption of small displacements and rotations of the components; and the neglect of effects such as those from the anti-roll bar, suspension geometry, and tire damping, which are assumed to have linear stiffness.

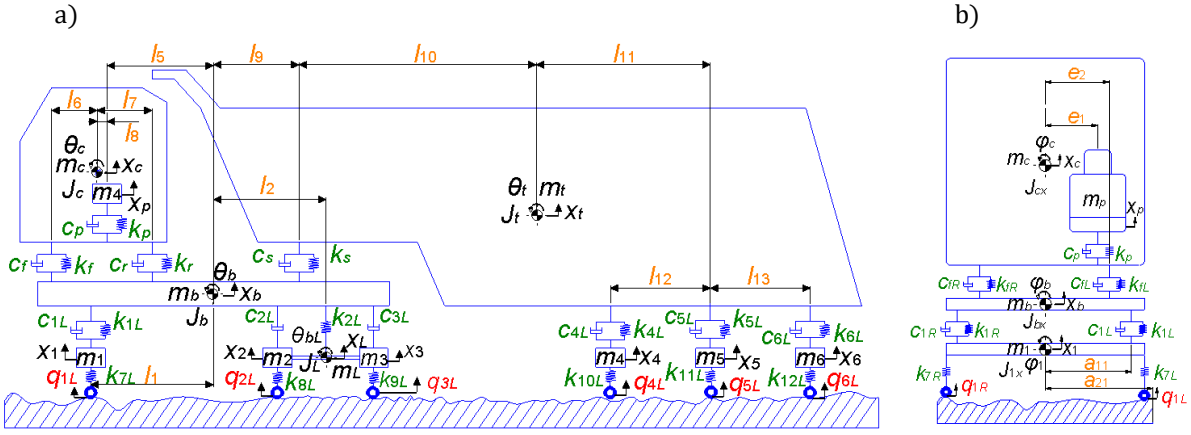


Figure 1. Tractor semi-trailer model: a) left side view, b) truck front view (Adapted from Chen *et al.*[3])

3.2 Biodynamic model

A 20-DOF biodynamic model was used to analyze the vibrations transmitted from the seat to the driver. The coupling between the human body and the seat surface is modeled by stiffness and damping, considering both the backrest and the human body inclined at 21°, as described by Kim et al. [1]. The efficient selection of a seat angle is an important factor that directly influences injuries, especially under certain impact conditions, as noted by Xiao *et al.* [5].

This multibody model considers 10 distinct mass segments: head (m_1), thorax (m_2), abdomen (m_3), pelvis (m_4), left upper arm (m_5), left forearm (m_6), left hand (m_7), right upper arm (m_8), right forearm (m_9), and right hand (m_{10}). Each mass segment has 2 DOFs—one for vertical displacement (z) and another for horizontal displacement (x), totaling 20 DOFs. The model is composed of 16 springs and dampers, characterized by their stiffness and damping parameters. The inter-segmental stiffness and damping are organized into 20×20 matrices, which include direct and cross-coupled parameters, and are used to analyze the system's vibrations.

The stiffness values, expressed in the vertical (k_{zz}) and longitudinal (k_{xx}) directions, as well as their coupling ($k_{xz} = k_{zx}$), were obtained from the study by Guruguntla and Lal [2]. Figure 2 represents the multibody model, although it visually shows only the stiffness components, the dampers are present in the model but are not explicitly displayed.

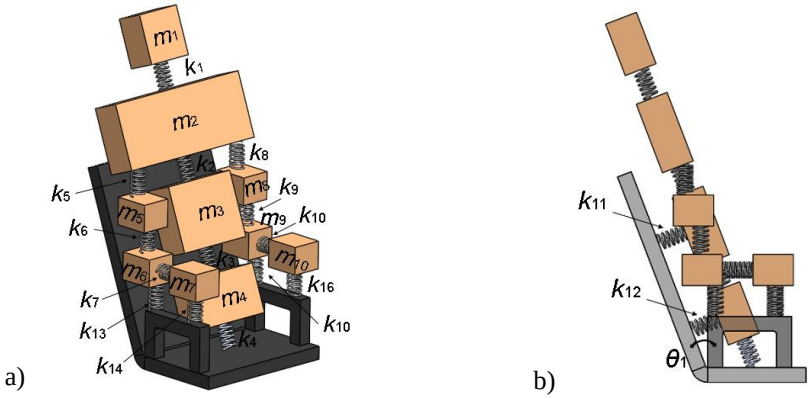


Figure 2. Biodynamic 20-DOF model: a) isometric view b) side view (Adapted from Guruguntla and Lal [2])

Equations (10) and (11) represent the dynamic equilibrium of the i^{th} segment of mass m_i, which is connected to the $(i+1)^{th}$ body segment. The equivalent force terms associated with the damping and stiffness elements in the longitudinal (x) and vertical (z) directions are included accordingly. Equation (12) consolidates these two expressions into a compact matrix form.

$$m_i\ddot{x}_i + c^i_{xx}(\dot{x}_i - \dot{x}_{i+1}) + c^i_{xz}(\dot{z}_i - \dot{z}_{i+1}) + k^i_{xx}(x_i - x_{i+1}) + k^i_{xz}(z_i - z_{i+1}) = f_{xi} \tag{10}$$

$$m_i\ddot{z}_i + c^i_{zx}(\dot{x}_i - \dot{x}_{i+1}) + c^i_{zz}(\dot{z}_i - \dot{z}_{i+1}) + k^i_{zx}(x_i - x_{i+1}) + k^i_{zz}(z_i - z_{i+1}) = f_{zi} \tag{11}$$

$$\mathbf{M}_i\ddot{\mathbf{p}}_i + \mathbf{C}_i\{\dot{\mathbf{p}}_i - \dot{\mathbf{p}}_{i+1}\} + \mathbf{K}_i\{\mathbf{p}_i - \mathbf{p}_{i+1}\} = \mathbf{f}_i \tag{12}$$

$$\mathbf{M}_i = \begin{bmatrix} m_i & 0 \\ 0 & m_i \end{bmatrix}, \mathbf{C}_i = \begin{bmatrix} c^i_{xx} & c^i_{xz} \\ c^i_{zx} & c^i_{zz} \end{bmatrix}, \mathbf{K}_i = \begin{bmatrix} k^i_{xx} & k^i_{xz} \\ k^i_{zx} & k^i_{zz} \end{bmatrix}, \mathbf{f}_i = \begin{Bmatrix} f_{xi} \\ f_{zi} \end{Bmatrix}, \mathbf{p}_i = \begin{Bmatrix} x_i \\ z_i \end{Bmatrix} \tag{13}$$

Equation (14), which represents the global equation of motion, describes the complete biodynamic system, where the global mass $\mathbf{M}$, damping $\mathbf{C}$, and stiffness $\mathbf{K}$ matrices are assembled by coupling all segmental matrices.

$$\mathbf{M}_{10x10}\ddot{\mathbf{p}}_{10x1} + \mathbf{C}_{10x10}\dot{\mathbf{p}}_{10x1} + \mathbf{K}_{10x10}\mathbf{p}_{10x1} = \mathbf{f}_{10x1} \tag{14}$$

To analyze the system in the frequency domain, a harmonic solution is assumed for both displacements and forces in eq. (14), resulting in eq. (15), which expresses the system in terms of complex amplitudes (P and F) and enables the evaluation of its frequency response. Equation (16) defines the vibration transmissibility between the seat and the head (TR_{Head}). This parameter could be expressed as the ratio between the vibratory response measured at the head ($Z_1 \sin\theta_1$) and the excitation input at the seat (Z_0).

$$(-\omega^2\mathbf{M} + j\,\omega\mathbf{C} + \mathbf{K})_{10x10}\mathbf{P}_{10x1} = \mathbf{F}_{10x1} \tag{15}$$

$$TR_{Head} = \frac{Z_1 \sin\theta_1}{Z_0} \tag{16}$$

The vertical-axis transmissibility between the seat and the head is evaluated to identify their displacements, as reported by Yu *et al.* [6]. The biodynamic behavior is influenced by the seat characteristics, and these properties determine how vibrations are transmitted to the human body, as described by Zhang *et al.* [7]. For this study, the mass values of each segment of the biodynamic model, as obtained from Guruguntla and Lal [2], are listed in Tab. 1.

Table 1. Mass values of the biodynamic model

Mass (kg)									
m_1	7.1	m_3	13.6	m_5	3.1	m_7	0.6	m_9	1.8
m_2	16.4	m_4	11.2	m_6	1.8	m_8	3.1	m_{10}	0.6

4 Vibration modes analysis

Modal analysis is performed to determine the natural vibration frequencies of the biodynamic model, that is, the frequencies at which the body tends to oscillate when subjected to external excitations.

Figures 3 and 4 present the vibration modes of the system, showing how the ten mass segments move when excited at their first three natural frequencies.

The vibration modes in the vertical direction are analyzed in Fig. 3. The first vibration mode represents the global vertical motion of the body, in which all segments move almost in phase. The second mode corresponds to a flexural motion between the seat and the upper body, indicating relative movement of the trunk with respect to the pelvis. The third mode is associated with localized vibration of the upper body, particularly the head and shoulders, oscillating over the trunk.

Figure 4 illustrates the longitudinal vibration modes of the biodynamic model. In the first mode, the body exhibits an overall forward–backward motion, with most segments moving almost in phase and showing minimal relative deformation. The second mode shows a pronounced longitudinal flexion, with the abdomen (m3) presenting the largest amplitude, indicating that this region acts as the main deformation point between the pelvis and the upper body. The third mode is dominated by localized longitudinal oscillations of the upper segments, particularly the head and thorax, relative to the abdomen, which typically occur at higher frequencies.

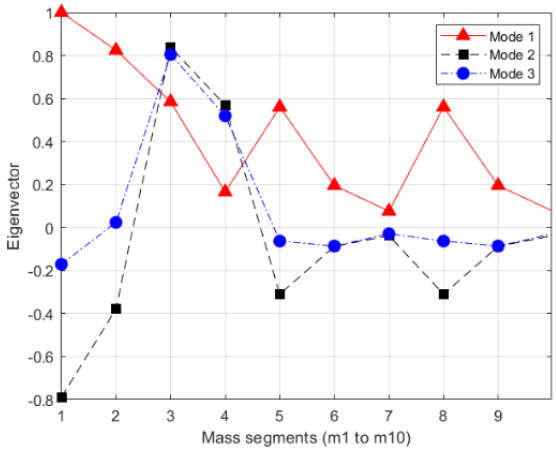


Figure 3. Vertical behavior of the masses in the first three vibration modes

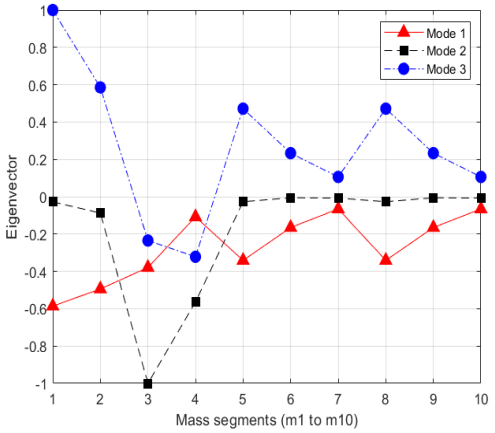


Figure 4. Longitudinal behavior of the masses in the first three vibration modes

5 Results of segmental transmissibility

Figures 5 and 6 show the vibration transmissibility from the vehicle seat to the driver's head and pelvis, respectively, with different behaviors for each body segment in the vertical axis.

Figure 5, corresponding to the transmissibility analysis for the head, shows a resonance peak at a higher frequency. At this point, head vibration is amplified, becoming greater than that of the seat. After the peak, the system behaves as an isolator, attenuating the vibrations.

Figure 6, representing the pelvis analysis, shows a lower resonance frequency. The phase plot in this case demonstrates an abrupt change and a large phase shift, which is expected since it is more directly connected to the seat. This behavior indicates that the system acts as a more effective isolator at higher frequencies for this region.

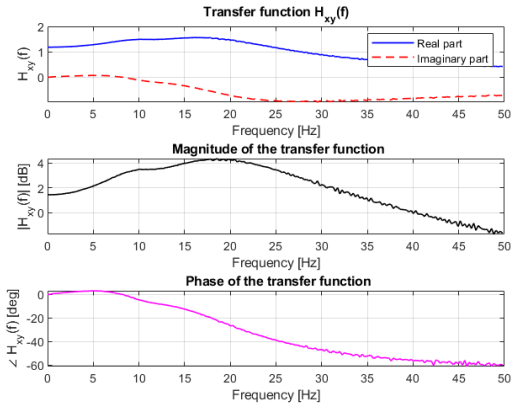


Figure 5. Transfer function response from the seat to the driver's head

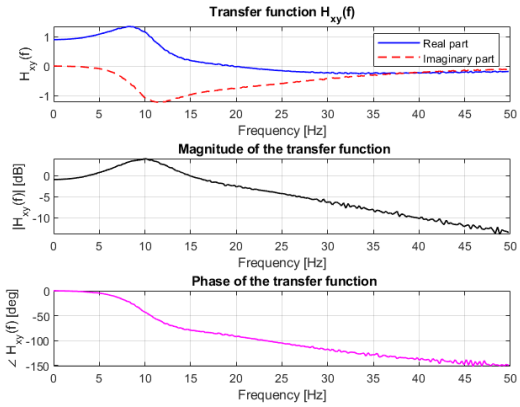


Figure 6. Transfer function response from the seat to the driver's pelvis

6 Conclusions

The modal analysis revealed that the biodynamic model exhibits distinct vibration modes in both vertical and longitudinal directions. The first modes are characterized by global body motions, while higher modes involve localized oscillations of specific segments, particularly in the upper body and head regions. These results highlight the importance of considering both global and segmental dynamics when evaluating vibration transmission and human body response.

The transmissibility analysis demonstrated that the vibration response varies significantly among body segments. The head exhibits higher resonance frequencies and greater amplification, while the pelvis shows lower resonance frequencies and stronger coupling with the seat. These findings confirm that the human body acts as a complex, frequency-dependent system, with distinct vibration isolation characteristics across different regions.

Future work should focus on refining damping parameters and validating the model through experimental measurements under real driving conditions.

Acknowledgements. This study was carried out with the support of Brazilian funding agencies: Coordination for the Improvement of Higher Education Personnel (CAPES) - Financing Code 001, National Council for Scientific and Technological Development (CNPq), and Research Support Foundation of the State of Rio Grande do Sul (FAPERGS).

Authorship statement. The authors hereby confirm that they are the sole liable persons responsible for the authorship of this work, and that all material that has been herein included as part of the present paper is either the property (and authorship) of the authors, or has the permission of the owners to be included here.

References

[1] E. Kim, M. Fard and K. Kato. “A seated human model for predicting the coupled human-seat transmissibility exposed to fore-aft whole-body vibration”. *Applied Ergonomics*, vol. 84, art. no. 102929, 2020.
[2] V.Guruguntla, M. Lal. “Multi-body modelling and ride comfort analysis of a seated occupant under whole-body vibration”. *Journal of Vibration and Control*, vol. 29, pp 3078-3095. 2022.
[3] K. Chen, S. He, E. Xu, W. Zheng and R. Tang, “Ride comfort analysis and multivariable co-optimization of the commercial vehicle based on an improved nonlinear model”, *IEEE Access*, vol. 8, pp. 2732-2749, 2020.
[4] P. Múčka. “Simulated road profiles according to ISO 8608 in vibration analysis”. *Journal of Testing and Evaluation*, vol. 46, no. 1, pp. 405-418. 2019.
[5] H. Xiao, K. Wang, Y. Liu, Q. Guo, Y. Wen, and Z. Feng. “Nonlinear dynamic modeling and body injuries analysis of human/seat system under vertical impact”. *International Journal of Industrial Ergonomics*, vol. 95, art.no. 103450, 2023.
[6] Z. Yu, Q. Zhao, J. Yang, Y. Xia, and Y. Ma. “Uncoupled spatial biodynamic model for seated humans exposed to vibration-development and validation”. *International Journal of Industrial Ergonomics*, vol 85, art. no. 103171, 2021.
[7] X. Zhang, X. Song, X. Wang, P. Yu, Y. Qiu, and Y. Miao. “Predicting the seat transmissibility of a seat-occupant system exposed to the whole-body vibration with combined artificial neural network and genetic algorithm”. *International Journal of Industrial Ergonomics*, vol 103, art. no. 103627, 2024.